

NB QC-LDPC Coded QAM Signals with Optimized Mapping: Bounds and Simulation Results

Irina E. Bocharova^{1,2}, Boris D. Kudryashov^{1,2}, Evgenii P. Ovsyannikov³, and Vitaly Skachek²

¹University of Information Technologies, Mechanics and Optics
St. Petersburg, 197101, Russia

³State University of Aerospace Instrumentation
St. Petersburg, 190000, Russia
Email: eovs@mail.ru

²University of Tartu, Estonia
Email: {irinaboc, boriskud}@ut.ee
{vitaly.skachek}@ut.ee

Abstract

This paper studies specific properties of nonbinary low-density parity-check (NB LDPC) codes when used in coded modulation systems. The paper is focused on the practically important NB LDPC codes over extensions of the Galois field $\text{GF}(2^m)$ with $m \leq 6$ used with QAM signaling. Performance of NB QC LDPC coded transmission strongly depends on mapping of nonbinary symbols to signal constellation points. We obtain a random coding bound on the maximum-likelihood decoding error probability for an ensemble of random irregular NB LDPC codes used with QAM signaling for specific symbol-to-signal point mappings. This bound is based on the ensemble average squared Euclidean distance spectra derived for these mappings. The simulation results for the belief-propagation decoding in the coded modulation schemes with the NB quasi-cyclic (QC)-LDPC codes under different mappings are given. Comparisons with the optimized binary QC-LDPC codes in the WiFi and 5G standards, as well as with the new bound, are performed.

I. INTRODUCTION

Nonbinary (NB) LDPC block codes over extensions of the binary Galois field were introduced in [3]. Since that time, the term *NB LDPC codes* is used for binary images of NB LDPC codes over extensions of the binary field [4], unlike the NB LDPC codes over arbitrary fields in [5]. In this paper, with a slight abuse of notations, we use the terms binary images of NB LDPC codes and NB LDPC codes interchangeably.

A. NB LDPC codes with small alphabets

The advantage of NB LDPC codes compared to their binary counterparts when used with QAM signaling in the AWGN channel was demonstrated in a number of papers (see, for example, [6], [7], [8] and references therein). In optimization of NB LDPC codes with both BPSK and QAM signaling, the most attention was paid to so-called ‘ultra-sparse’ regular codes, that is, the regular codes with only two nonzero elements in each column of their parity-check matrices. Mainly the Galois field extensions $\text{GF}(2^m)$ with $m \geq 6$ were considered since it was shown by simulations of NB LDPC codes of short and moderate lengths that increasing m improves the performance of iterative decoding. The belief-propagation (BP) decoding thresholds for ultra-sparse regular NB LDPC codes used in the AWGN

Parts of this work were presented at the IEEE ISIT 2021 [1] and ITW 2021 [2].

The work of I.E. Bocharova, B.D. Kudryashov and V. Skachek is supported in part by the grant PRG49 from the Estonian Research Council. The work of V. Skachek is also supported in part by the ERDF via CoE project EXCITE. The work of I.E. Bocharova, B.D. Kudryashov and E.P. Ovsyannikov is also supported in part by the Ministry of Science and Higher Education of Russian Federation, project no. 2019-0898.

channel as a function of m were presented in [4] and [9]. It was shown that BP decoding thresholds for the AWGN channel strongly depend on the field size and are much smaller for $m \geq 6$ than those for smaller m , although in the general, behavior of the thresholds may not be a monotonic function. However, increasing m leads to the higher computational complexity of BP decoding. This draws attention to looking at NB LDPC codes over smaller fields to find a trade-off between performance and complexity.

NB LDPC codes with QAM signaling for small field sizes, that is, for $m = 2, \dots, 5$ were considered in a limited number of papers. It was discovered through the analysis by density evolution technique as well as simulations in [10] that for small $m < 6$, the average column weight of NB LDPC code base matrix should be around the interval [2.2, 2.4]. In the same paper, BP decoding thresholds for rate $1/2$ ‘semi-regular’ NB LDPC codes over $\text{GF}(2^m)$, $m = 2, \dots, 6$ were derived. The authors concluded that if column weight is larger than 3, the thresholds for small field sizes are better than for large ones, while for column weight smaller than 2.5, performance improves with increasing m . In [11], experimental results for high-rate regular NB QC-LDPC codes over $\text{GF}(2^2)$, $\text{GF}(2^3)$, and $\text{GF}(2^4)$ used for optical communications were presented. High-rate irregular NB LDPC codes were studied in [12]. It was noticed in this paper that high-rate NB LDPC codes with three nonzero elements in each column of their parity-check matrix are superior to ultra-sparse NB LDPC codes if the alphabet size is small.

In [13], an approach for optimization of NB QC LDPC block codes over $\text{GF}(2^m)$ for $m \leq 6$ was suggested. It is based on applying the simulated annealing technique [14] to constructing the code base matrix followed by optimization of the degree matrix performed by the algorithm in [15]. In the same paper, an ensemble of irregular NB LDPC codes determined by the parity-check matrix with column weights two and three was introduced and analyzed. A finite-length random coding bound on the maximum-likelihood (ML) decoding performance for this ensemble of codes used with BPSK signaling in the AWGN channel was derived.

The improvement in the performance of NB LDPC codes over their binary counterparts comes at the cost of higher decoding complexity. In the general case, the generalized belief propagation (BP) decoding complexity per bit for a binary image of the NB LDPC code is proportional to q^2 , where $q = 2^m$. However, implementation of the decoder based on the fast Hadamard transform (FHT) has complexity proportional to $q \log_2 q$ (see, for example, [16]). Moreover, there exist simplified decoding techniques such as, for example, extended min-sum (EMS) algorithm proposed in [17], [16], or Min-Max decoding in [18], [19], which allow to significantly reduce the decoding complexity at the cost of relatively small losses in the decoding performance (≈ 0.2 dB). According to the published results regarding VLSI implementation complexity [20], simplified decoding of NB LDPC codes over $\text{GF}(2^4)$ is a few times more complex than the decoding of binary codes of the same rate and binary length with the same throughput of the decoder.

B. Matching NB LDPC codes with QAM modulation

It was shown (see, for example, [6]) that compared to the binary LDPC codes used with QAM signaling, the performance of NB LDPC codes used with QAM signaling is much more influenced by the choice of code symbol-to-QAM signal mapping. This, typically, restricts the number of admissible pairs (m, M) used both in practical schemes and theoretical studies. In particular, in [6], regular NB LDPC codes over $\text{GF}(2^m)$ with M^2 -QAM signaling, where either $\log_2 M = m$ or $\log_2 M$ is a divisor of m , were considered.

Since QAM signals are represented by two orthogonal PAM-signal components, the achievable transmission rate for QAM signaling in the AWGN channel is precisely two times larger than for PAM signaling with the same signal-to-noise ratio per signal component. In the survey below, we do not distinguish between research results for QAM and PAM meaning that results obtained for M -PAM signaling can be easily reformulated for M^2 -QAM signaling.

There are two main techniques for matching outputs of a binary LDPC encoder with inputs of the QAM modulator: bit-interleaved coded modulation (BICM) [21] and multi-level coding (MLC) [22]. When using BICM, the encoded bits are interleaved and mapped, typically according to a Gray mapping, to signal constellation points. The MLC mapping can be considered as a generalization of trellis-coded modulation (TCM) introduced in [23]. When applying this technique, the input bits are split into groups, and bits inside each group can be encoded by different codes or left uncoded. Then the encoded bits of the same group are mapped into appropriate signal constellation points.

In order to match the NB LDPC code with QAM signals besides BICM, symbol interleaved modulation (SICM), as in [6], [7] and [12], is used. In this case, symbols of an NB LDPC code are interleaved and then mapped to modulation signals.

This paper is organized as follows. In Section II, necessary definitions are given. QAM modulation and demodulation schemes in combination with BP decoding for irregular NB LDPC codes over small alphabets are studied in Section III. In Section IV, we consider an ensemble of random irregular NB LDPC codes and a random binary image of this ensemble used with the QAM signaling and different mappings in the AWGN channel. The average squared Euclidean distance spectra (SEDS) for these two ensembles are derived and discussed in the same section. A finite-length random coding bound on ML decoding error probability for the ensemble of irregular NB LDPC codes based on its SEDS is obtained. Simulation results of the FER performance of the BP decoding for the NB QC-LDPC codes, optimized as in [13], are presented and compared with the theoretical bound in Section V. The paper is concluded by a short discussion. For completeness, a known bound on the error probability of ML decoding is presented in Appendix.

The main contributions of the paper are:

- The new modulation-demodulation schemes suitable for any pairs of parameters (m, M)
- Average squared Euclidean distance spectra for the ensemble of irregular NB LDPC codes used with BICM and SICM mappings
- A finite-length random coding bound on the error probability of ML decoding for the ensemble of irregular NB LDPC codes used with QAM signaling and different mappings in the AWGN channel

II. PRELIMINARIES

A rate $R = b/c$ NB QC-LDPC code over $\text{GF}(2^m)$ is defined by its polynomial parity-check matrix of size $(c - b) \times c$

$$H(D) = \{h_{ij}(D)\},$$

where $h_{ij}(D)$ are polynomials of formal variable D with coefficients from $\text{GF}(2^m)$. In the sequel, $h_{ij}(D)$ are either zeros or monomials and

$$H(D) = \{\alpha_{ij}D^{w_{ij}}\}, w_{ij} \in \{0, 1, \dots, \nu\}, \alpha_{ij} \in \text{GF}(2^m), i = 1, \dots, c - b, j = 1, \dots, c,$$

where ν denote the maximal degree of a monomial. The corresponding q -ary parity-check matrix, $q = 2^m$ of the (Lc, Lb) NB QC-LDPC block code is obtained by replacing $D^{w_{ij}}$, by the w_{ij} -th power of a circulant permutation matrix of order L . The parameter L is called *lifting factor*. The parity-check matrix in binary form which determines *binary image* of the NB LDPC code is obtained by replacing non-zero elements of the q -ary, $q = 2^m$ parity-check matrix by binary $m \times m$ matrices, which are companion matrices of the corresponding field elements [24].

Let $\alpha_i = (\alpha_{i1}, \alpha_{i2}, \dots, \alpha_{iw_i})$ be a vector consisting of nonzero elements of i th row of $H(D)$ and w_i be the number of nonzero elements of this row. After replacing these nonzero elements with their binary $m \times m$ companion matrices, we obtain an $m \times mw_i$ parity-check matrix of a linear code which we call the i -th *constituent* code of the NB LDPC code.

To facilitate the low encoding complexity, we consider parity-check matrices having the form (see, for example, [15])

$$H(D) = (H_{\text{inf}}(D) \quad \mathbf{h}_0(D) \quad H_{\text{bd}}(D)), \quad (1)$$

where $H_{\text{bd}}(D)$ is a bidiagonal matrix of size $(c-b) \times (c-b-1)$, $\mathbf{h}_0(D)$ is a column with two nonzero elements, and $H_{\text{inf}}(D)$ can be any monomial submatrix of size $(c-b) \times b$. This submatrix corresponds to the information part of a codeword.

Binary matrix $B = \{b_{ij}\}$ of the same size as $H(D)$ is called *base matrix* for $H(D)$ if $b_{ij} = 1$ iff $h_{ij}(D) \neq 0$.

In the search for optimized parity-check matrices, we represent $H(D)$ in the form of two matrices: degree matrix $H_w = \{w_{ij}\}$ and matrix of field coefficients $H_c = \{\alpha_{ij}\}$ which we obtain by labeling nonzero elements of B by monomial degrees and nonzero field elements, respectively. In these matrices only elements for which elements of base matrix $b_{ij} = 1$ are meaningful. For that reason, in H_w and H_c we write “-1” in positions corresponding to zero elements of B .

For example, the rate $R = 1/4$ NB QC-LDPC code over $\text{GF}(2^4)$ determined by

$$H(D) = \begin{pmatrix} D^0 & D^0 & D^0 & D^0 \\ D^0 & \alpha D^3 & 0 & \alpha^3 D^7 \\ D^0 & \alpha^2 D^9 & \alpha^5 D^2 & \alpha^{11} D \end{pmatrix}$$

has the following matrices H_w and H_c

$$H_w = \begin{pmatrix} 0 & 0 & 0 & 0 \\ 0 & 3 & -1 & 7 \\ 0 & 9 & 2 & 1 \end{pmatrix},$$

$$H_c = \begin{pmatrix} 1 & 1 & 1 & 1 \\ 1 & \alpha & -1 & \alpha^3 \\ 1 & \alpha^2 & \alpha^5 & \alpha^{11} \end{pmatrix},$$

where α is a primitive element of $\text{GF}(2^4)$. The corresponding matrix B is

$$B = \begin{pmatrix} 1 & 1 & 1 & 1 \\ 1 & 1 & 0 & 1 \\ 1 & 1 & 1 & 1 \end{pmatrix}.$$

Notations used throughout the paper are summarized in Table I.

III. MAPPINGS OF NB LDPC CODE SYMBOLS TO QAM SIGNALS

In order to provide for better matching of the PAM signals with the NB LDPC codes, one should take into account the fact that the sign and the amplitude bits of the PAM signals have different significance. This property makes the error-correcting capability of the NB LDPC codes sensitive to the mapping of the code symbols onto the PAM signals. Next, we consider four modulation schemes matched with NB LDPC coding.

A. PAM mapper-modulators

Let n be the codeword length in bits. Suppose that both m and $p = \log_2 M$ are divisors of n , that is, $N = n/m$ and $N_p = n/p$ are integers. Four modulation schemes matched with non-binary coding are presented in Fig. 1. The modulator A performs a bit-interleaved mapping (BICM), that is, codeword bits v_{11}, v_{12}, \dots corresponding to $N = n/m$ 2^m -ary symbols are split into groups of $p < m$ bits, where the first bit of each group (S -bit) is mapped onto the sign of the 2^p -PAM signal and the other bits (A_1, A_2, \dots, A_{p-1}) determine the amplitude of the corresponding 2^p -PAM signal. Modulator A can be

TABLE I: Notations

Notation	Comment
b	Number of rows in the base matrix
$c - b$	Number of columns in the base matrix
$B = \{b_{ij}\}, i = 1, \dots, c - b, j = 1, \dots, c$	Base matrix
D	Formal variable
$H_w = \{w_{i,j}\}, i = 1, \dots, c - b, j = 1, \dots, c$	Degree matrix, $w_{ij} = -1$ corresponds to zero entry in B
$H_c = \{\alpha_{i,j}\}, i = 1, \dots, c - b, j = 1, \dots, c$	Matrix of coefficients, $\alpha_{ij} = -1$ corresponds to zero entry in B
$q = 2^m$	Size of extension of the Galois field
$n, k, r = n - k$	Codelength, number of information symbols and number of redundant bits
$N = \frac{n}{m}$	Codelength in symbols of GF(q)
$M = 2^p$	PAM modulation order. It corresponds to M^2 -QAM
$N_p = \frac{n}{p}$	Length of codeword in PAM signals
$L = \frac{n}{K}$ or $L = \frac{n}{K} = \frac{r}{J}$	Lifting factor of QC-LDPC code or strip size for Gallager's ensemble
$(J, K)^c$	Column and row weight for regular LDPC code
$\mathcal{L}(\cdot)$	Log-likelihood ratios for symbols and sequences
AE	Signal alphabet extension
ASCM	Amplitude-sign coded modulation
BICM	Bit-interleaved coded modulation
BPCM	Bit-plane coded modulation
CGF	Combinatorial generating function
MGF	Moment generating function
SICM	Signal-interleaved coded modulation
SEDS	Squared Euclidean distance spectrum
SED	Squared Euclidean distance

used for any pair (m, p) . If this mapping is used, typically, code symbols are not equally reliable due to an arbitrary mapping of their bits onto signs and amplitudes of the PAM signals.

Modulator B implements symbol-interleaved mapping (SICM). It is applicable only if p is either equal to m or is a divisor of m . We consider the latter case. Then each group of m bits corresponding to the 2^m -ary symbol is split into a few groups of p bits. The first bit in each group determines the sign of the 2^p -PAM signal, and the other bits of each group are mapped onto the PAM signal amplitude. Thus, a certain fixed number of sign bits are combined with a certain number of amplitude bits. This makes all code symbols equally reliable.

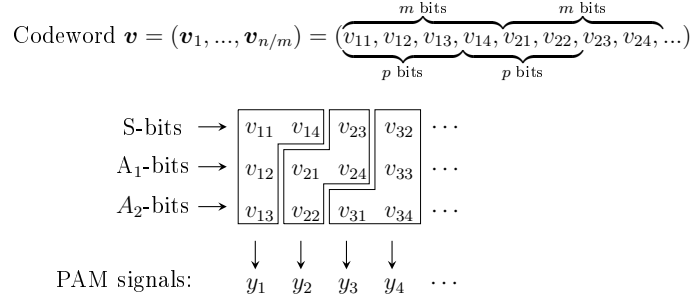
The next two new mappings do not require p to be a divisor of m and can be applied to a large set of parameters m and p . We show both by comparing theoretical ML decoding error probability bounds and by simulating BP decoding that, unlike the BICM, these mappings used with *modified* demodulators contribute to better decoding performance.

Now assume that $p > m$, m is not required to be a divisor of p . The modulator C performs “*a bit-plane mapping*” (BPCM), which assumes that the first, the $(p + 1)$ -th, the $(2p + 1)$ -th, \dots group of m code bits are mapped onto the signs of the PAM signals, and other groups of m code bits are mapped onto the first, the second, \dots , the $(p - 1)$ -th amplitude bits of the PAM signals. The shortcoming of this mapping is that symbols consisting of sign (most significant) bits are more reliable than the other symbols consisting of amplitude (less significant) bits. However, if BPCM is used, the reliability distribution of the code symbols can be controlled both in the demodulator and at the code design level.

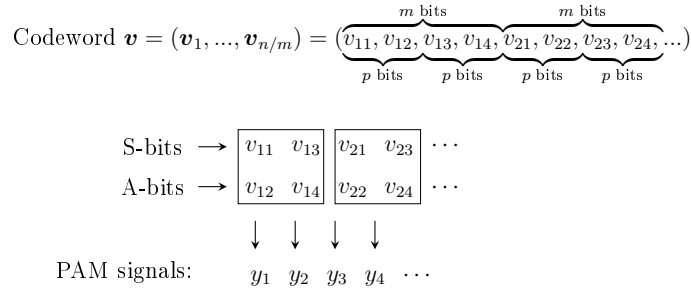
Mapping performed in the modulator D we call “*amplitude/sign mapping*” (ASCM). It is assumed that $p < m$ and $p - 1$ is a divisor of m , that is, $m = a(p - 1)$, a is an integer. The sign bits of the m PAM signals are formed as in BPCM. Then the first, the second, \dots , the $(p - 1)$ -th amplitude bits of the $a = m/(p - 1)$ PAM signals are formed. Similarly to BPCM, ASCM provides a possibility to control the code symbol reliabilities.

In the 2^p -PAM modulator, first, one of the four mappers (A–D in Fig. 1) is used to form p binary sequences: one sign bit sequence $\mathbf{s} = (s_1, s_2, \dots, s_{N_p})$ and $p - 1$ amplitude bit sequences

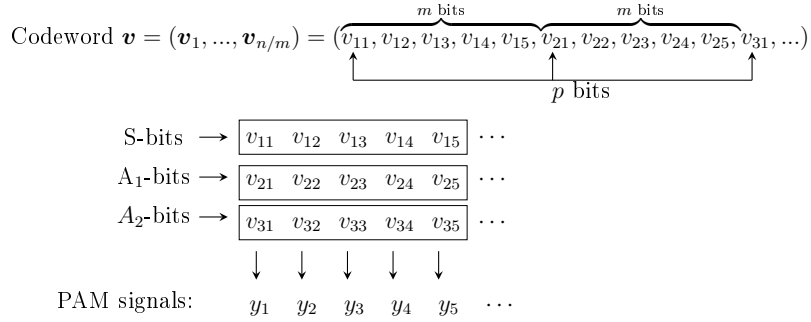
A: Bit-interleaved mapping (BICM), $\text{GF}(2^m) \rightarrow 2^p\text{-PAM}$, $m = 4$, $p = 3$



B: Symbol-interleaved mapping (SICM), $\text{GF}(2^m) \rightarrow 2^p\text{-PAM}$, $m = 4$, $p = m/2$



C: Bit-plane mapping (BPCM), $\text{GF}(2^m) \rightarrow 2^p\text{-PAM}$, $m = 5$, $p = 3$



D: A/S-mapping (ASCM), $\text{GF}(2^m) \rightarrow 2^p\text{-PAM}$, $p = 3$, $m = a(p - 1) = 4$, $a = 2$

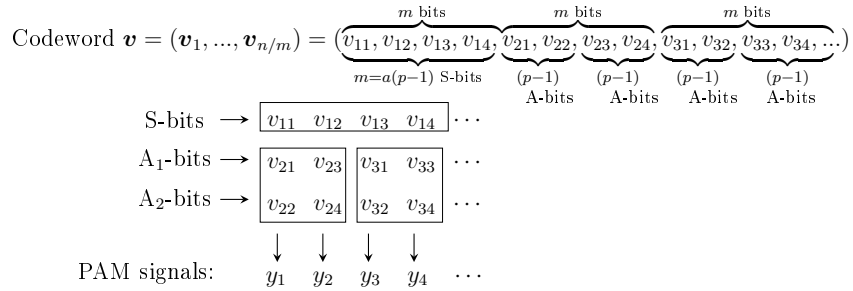


Fig. 1: Modulation techniques for matching outputs of NB LDPC codes over $\text{GF}(2^m)$ and 2^p-PAM signals, $p = \log_2 M$

TABLE II: Gray mapping amplitude to amplitude bits

Modulation order	Binary representation \mathbf{v} for amplitudes $A(\mathbf{v})$ of PAM signal points							
	1	3	5	7	9	11	13	15
4-PAM	1	0	–	–	–	–	–	–
8-PAM	10	11	01	00	–	–	–	–
16-PAM	110	111	101	100	000	001	011	010

$\mathbf{a}_i = (a_{i1}, a_{i2}, \dots, a_{iN_p})$, $i = 1, \dots, p-1$. Then, the PAM signal y_t is computed as

$$y_t = (2s_t - 1)A(a_{1t}, \dots, a_{(p-1)t}), \quad t = 1, 2, \dots, N_p,$$

where $A(\cdot)$ denotes the amplitudes of the signal points obtained according to the Gray mapping. An example of the Gray mapping used for 4-PAM and 8-PAM modulation is given in Table II.

The binary image of a 2^m -ary codeword $\mathbf{v} = (\mathbf{v}_1, \mathbf{v}_2, \dots, \mathbf{v}_N)$, $\mathbf{v}_i = (v_{i1}, \dots, v_{im})$ is mapped onto the signal sequence $\mathbf{y} = (y_1, y_2, \dots, y_{N_p})$, which is transmitted over the AWGN channel. The received sequence is

$$r_t = y_t + n_t, \quad t = 1, 2, \dots, N_p,$$

where the noise samples n_t are independent Gaussian variables with zero mean and variation $\sigma^2 = N_0/2$.

B. Demodulator-demappers

In this subsection, we show that for different mappings dependencies between NB code symbols and the corresponding PAM signals can be taken into account when computing symbol LLRs. A decoding performance gain can be obtained by using more informative outputs of the demodulator.

First, we revisit the demodulator for the BICM mapping and then show how the reliability of the 2^m -ary code symbol can be computed when the mapping onto a few PAM signals is applied. In the demodulator, first, LLRs of signal points are computed. We assume that signal points are equiprobable, then the a posteriori probabilities of signal points $\xi \in \{-2^p + 1, -2^p + 3, \dots, -1, 1, \dots, 2^p - 3, 2^p - 1\}$ given the channel output $\mathbf{r} = (r_1, \dots, r_{N_p})$ are

$$P(y_t = \xi | r_t) = K(r_t) \exp \left\{ -\frac{(r_t - \xi)^2}{N_0} \right\},$$

where $K(r_t)$ are probability normalizing coefficients providing $\sum_{\xi} P(\xi | r_t) = 1$. Next, a posteriori probabilities of bits in the binary representation of signal points are computed by summing up probabilities of signal points with zero and one in the corresponding positions. According to Table II, the log-likelihood ratios (LLRs) $\mathcal{L}(\cdot)$ of the sign and amplitude bits in the binary representation of the signal points ξ are computed as follows

$$\mathcal{L}(s | r_t) = \log \frac{P_{\xi \in \xi_{s,1}}(\xi | r_t)}{P_{\xi \in \xi_{s,0}}(\xi | r_t)} \quad (2)$$

$$\mathcal{L}(a_i | r_t) = \log \frac{P_{\xi \in \xi_{a_i,1}}(\xi | r_t)}{P_{\xi \in \xi_{a_i,0}}(\xi | r_t)}, \quad (3)$$

where $i = 1, \dots, p-1$,

$$\xi_{s,0} = \{-2^p + 1, -2^p + 3, \dots, -3, -1\},$$

$$\xi_{s,1} = \{1, 3, \dots, 2^p - 1\},$$

$$\xi_{a_1,0} = \{-2^p + 1, -2^p + 3, \dots, -2^{p-1} - 1, 2^{p-1} + 1, 2^{p-1} + 3, \dots, 2^p - 1\}.$$

$$\xi_{a_1,1} = \{-2^{p-1} + 1, -2^{p-1} + 3, \dots, -1, 1, 3, \dots, 2^{p-1} - 1\}.$$

For example, for 4-PAM used with the Gray mapping as in Table II, $\xi_{s,0} = \{-3, -1\}$, $\xi_{s,1} = \{1, 3\}$, $\xi_{a_1,0} = \{-3, 3\}$, $\xi_{a_1,1} = \{-1, 1\}$.

Signal sets $\xi_{a_i,0}$ and $\xi_{a_i,1}$ for $i \geq 2$ depend on the modulation index. For example, for 8-PAM $\xi_{a_2,0} = \{-5, -3, 3, 5\}$ and $\xi_{a_2,1} = \{-7, -1, 1, 7\}$. According to Table II, we have

$$\begin{aligned}\mathcal{L}(s|r_t) &= \log \frac{P(1|r_t) + P(3|r_t) + P(5|r_t) + P(7|r_t)}{P(-1|r_t) + P(-3|r_t) + P(-5|r_t) + P(-7|r_t)} \\ \mathcal{L}(a_1|r_t) &= \log \frac{P(-3|r_t) + P(-1|r_t) + P(1|r_t) + P(3|r_t)}{P(-7|r_t) + P(-5|r_t) + P(5|r_t) + P(7|r_t)} \\ \mathcal{L}(a_2|r_t) &= \log \frac{P(-5|r_t) + P(-3|r_t) + P(3|r_t) + P(5|r_t)}{P(-7|r_t) + P(-1|r_t) + P(1|r_t) + P(7|r_t)}.\end{aligned}\quad (4)$$

Computation of the LLRs for the NB code symbols \mathbf{v} depends on the mapping used. In the case of BICM, one, typically, ignores the symbol bits dependencies, and the LLRs of code symbols \mathbf{v} are computed as:

$$\mathcal{L}(\mathbf{v} = (v_1, \dots, v_m)|\mathbf{r}) = \sum_{i=1}^m \mathcal{L}(v_i|r_i). \quad (5)$$

When BICM is applied, if the bits are randomly permuted before mapping, expression (5) gives the correct LLR values.

If the bits of the 2^m -ary symbol are mapped onto a few PAM signals, then the amplitude bit dependencies can be taken into account. For BPCM, we compute the symbol LLRs as:

$$\mathcal{L}(\mathbf{v} = (v_1, \dots, v_m)|\mathbf{r}) = \sum_{i=1}^m \mathcal{L}(v_i|\mathbf{r}). \quad (6)$$

In terms of the sign and amplitude bits of the PAM signals we have

$$\mathcal{L}(\mathbf{v}_j|\mathbf{r}) = \sum_{i=1}^m \mathcal{L}(v_{ji}|\mathbf{r}), \quad v_{ji} = \begin{cases} s_{(j-1)m+i}, & j = 1, p+1, \dots, N-p+1 \\ a_{\ell, (j-1-\ell)m+i}, & j = \ell+1, \ell+p+1, \dots, N-p+\ell+1 \end{cases},$$

$j = 1, 2, \dots, N$, $\ell = 1, 2, \dots, p-1$, $s_{(j-1)m+i}$ and $a_{\ell, (j-1-\ell)m+i}$ denote the sign bit of the $((j-1)m+i)$ -th PAM signal and the ℓ -th amplitude bit of the $((j-1-\ell)m+i)$ -th PAM signal, $\ell = 1, 2, \dots, p-1$.

For SICM and ASCM, the symbol LLRs for SICM and LLRs of all symbols except for those corresponding to sign bits in the cas of ASCM can be expressed as follows:

$$\mathcal{L}(\mathbf{v}) = \sum_{i=1}^{\beta} \mathcal{L}(v_i, v_2, \dots, v_{i+\alpha-1}|\mathbf{r}),$$

where

$$\begin{aligned}\beta &= \begin{cases} m/p & \text{for SICM} \\ a & \text{for ASCM} \end{cases}, \\ \alpha &= \begin{cases} p & \text{for SICM} \\ p-1 & \text{ASCM} \end{cases}\end{aligned}$$

and the number of components in \mathbf{r} depends on the choice of the mapping and the pair (p, m) .

The following two examples provide solutions for particular choices of the parameters p and m .

Example 1: Consider 4-PAM signaling used with SICM, and let $m = 4$ as in Fig. 1. The LLR of the q -ary symbol $\mathbf{v} = (v_1, v_2, v_3, v_4)$ transmitted by 4-PAM signals y_1 and y_2 can be computed as

$$\mathcal{L}(\mathbf{v} = (v_1, \dots, v_4|r_1, r_2)) = \sum_{i=1}^2 \mathcal{L}(v_{2i-1}, v_{2i}|r_i), \quad (7)$$

where

$$\mathcal{L}(v_{2i-1}, v_{2i}|r_i) = \log K(r_i) + \log \left(\exp \left\{ -\frac{((2v_{2i-1} - 1)A(y_i) - r_i)^2}{N_0} \right\} \right), i = 1, 2,$$

where $K(r_j)$ is a probability normalization coefficient, $A(y_i)$ denotes the amplitude of the i -th signal chosen according to Table II.

Example 2: Consider 8-PAM signaling with ASCM and let $m = 4$ as in Fig. 1. In this case, the LLRs for symbols associated with the sign bits are computed according to (2) and (6). Let $\mathbf{v} = (v_1, v_2, v_3, v_4)$ be a code symbol corresponding to the amplitude bits of two 8-PAM signals, y_1 and y_2 . We assume that signs are equiprobable. Then the average (over equiprobable signs) conditional probabilities of amplitude bit pairs (v_{2i-1}, v_{2i}) are equal to

$$\begin{aligned} P(v_{2i-1}, v_{2i}|r_i) &= K(r_i) \left(\exp \left\{ -\frac{(A(y_i) - r_i)^2}{N_0} \right\} \right. \\ &\quad \left. + \exp \left\{ -\frac{(-A(y_i) - r_i)^2}{N_0} \right\} \right), i = 1, 2. \end{aligned}$$

The LLR for the code symbol \mathbf{v} is computed according to (7), where

$$\mathcal{L}(v_{2i-1}, v_{2i}|r_i) = \log K(r_i) + \log \left(\sum_{j=1}^2 \exp \left\{ -\frac{((-1)^j A(y_i) - r_i)^2}{N_0} \right\} \right).$$

The last two examples show that for some modulation schemes, it is possible to compute LLRs for symbols with taking into account dependencies between reliabilities of bits in the binary image of this code symbol. Simulation results presented in Section V show that using a mapping that better matches the output of the NB LDPC code encoder to the PAM signal modulator/demodulator, the decoding efficiency of the NB LDPC codes can be improved. In the next section, we compare a random coding bound on the ML decoding performance computed for the ensemble of NB LDPC codes used with QAM signaling and different mappings.

IV. RANDOM CODING BOUND FOR THE ENSEMBLE OF ALMOST REGULAR NB LDPC CODES

The most often used lower bound on the error probability of ML decoding of block codes over the AWGN channel is the Shannon bound [25]. This bound cannot be used for PAM-modulated signals since all codewords in the Shannon bound have to be of the same energy. Most of upper bounds (see e.g. [26], [27]) use the same assumption. An upper bound which is valid for arbitrary signal sets is presented in [28].

Most of upper bounds are the union-type bounds and require for computation to know the code weight enumerators. For a long LDPC code it is computationally infeasible to find the weight enumerators. An approach to avoid this problem was suggested by R. Gallager in his famous book [5], where he considered a random ensemble of regular LDPC codes and derived the average over the ensemble code spectrum. Further we follow the same approach.

In this section, we compute the Herzberg-Poltyrev (HP) upper bound in [28] on the error probability of ML decoding for the random ensemble of ‘‘almost regular’’ NB LDPC codes in [13] used with PAM signaling. For completeness of the paper, we present the corresponding upper bound in the Appendix A.

The average binary Hamming weight spectrum for the ensemble of almost regular NB LDPC codes with two and three nonzero elements in each column of their parity-check matrix was derived in [13], where a finite-length random coding bound on ML decoding error probability of NB LDPC codes used with BPSK signaling was computed. In order to compute bound (25) in the case of PAM signaling it is necessary to know the SEDS of the code. We aim at finding the relation between the Hamming weight enumerators and the SEDS for the ensemble in [13].

In this section, we survey the existing ensembles of binary and NB LDPC codes. Then the average SEDS for the ensemble of irregular NB LDPC codes in [13] used with SICM and BICM, ASCM, or BPCM mappings are derived via the average Hamming distance spectra of this NB code ensemble and its binary image, respectively.

A. Ensembles of NB LDPC codes

Various ensembles of irregular binary LDPC codes were studied in [29], [30], and in [31]. A generalization of the ensemble in [30] to an ensemble of NB LDPC over $\text{GF}(2^m)$ determined by the ensemble of irregular bipartite graphs with given degree distributions on variable and check nodes, where each edge is labeled by an element of $\text{GF}(2^m)$, was studied in [32]. In particular, the average symbol Hamming weight and bit Hamming weight spectra of the random ensemble of irregular NB LDPC codes were derived.

However, for finite-length analysis both the ensemble of irregular binary LDPC codes in [29], [30] and its generalization to the nonbinary case in [32] have the same shortcoming. They do not determine irregular codes with predetermined column and row weight distributions. Due to unavoidable parallel edges in the code Tanner graph, the true degree distributions may differ from the expected one, and this phenomenon complicates the finite-length analysis of the ensemble. The finite-length analysis for the ensemble in [31] is even more difficult. Asymptotic generating functions for code Hamming weight spectra were found in [31]. Ensembles of both binary and NB regular LDPC codes were first analyzed by Gallager in [5]. Later, a few different ensembles of binary LDPC codes were studied in [33].

For the Gallager ensemble of binary (J, K) -regular codes, the parity-check matrix for a code with design rate $R = 1 - J/K$ consists of J strips $H_b^T = (H_{b,1}^T | H_{b,2}^T \dots | H_{b,J}^T)^T$, where each strip $H_{b,i}$ of width $L = r/J$ is a random permutation of the first strip which can be chosen in the form

$$H_{b,1} = \underbrace{(I_L \dots I_L)}_K,$$

where I_L is the identity matrix of order L .

Average Hamming weight spectra for the corresponding ensembles of regular LDPC codes were derived in [5] and [33]. In [34], asymptotic average Hamming weight spectra for ensembles of regular NB LDPC codes over $\text{GF}(2^m)$ were obtained. In [35], we presented a low-complexity recurrent procedure for computing exact Hamming weight spectra of both binary and NB random ensembles of regular LDPC codes.

As was mentioned before, for NB LDPC codes over small alphabets, the average column weight of the parity-check matrix around the interval [2.2, 2.4] is preferable. This is the reason for focusing on the ensemble of “almost regular” NB LDPC codes in this paper.

The ensembles of almost regular binary and NB LDPC codes with only two and three nonzero elements in each column of their parity-check matrices were considered in [13]. In the same paper, the low-complexity procedure for computing the average Hamming weight spectra in [35] was applied to compute the corresponding spectra for these ensembles. The ensemble of NB LDPC codes in [13] is based on the binary ensemble obtained from the Gallager ensemble of binary LDPC codes by allowing a given number $K_i \leq K$ of identity matrices and $K - K_i$ of all-zero $L \times L$ submatrices $\mathbf{0}_L$ in strips. Without loss of generality the i th strip can be chosen as random permutation $\pi_i(H_{b,i})$ where $H_{b,i}$ has the form

$$H_{b,i} = \underbrace{(I_L \dots I_L)}_{K_i} \underbrace{\mathbf{0}_L \dots \mathbf{0}_L}_{K-K_i}, \quad i = 1, \dots, J. \quad (8)$$

That is, the strips in the generalized ensemble are permuted versions of Gallager’s strip with some identity matrices replaced by the all-zero matrices of the same order. By choosing K_i , we adjust the column weight and row weight distributions. The corresponding random ensemble of NB LDPC codes

is determined by the parity-check matrix (8) whose nonzero entries are labeled by randomly chosen elements of $\text{GF}(2^m)$. We denote the labeled parity-check matrix by H_L . We refer to this NB ensemble as \mathcal{N} .

The straightforward method for constructing a binary image of the ensemble of NB codes is replacing the elements of $\text{GF}(2^m)$ in the labeled matrix H_L by the corresponding binary $m \times m$ companion matrices of the field elements. Thus, we obtain binary strips of size $Lm \times n$. All J strips of the random matrix are generated as one of $n!$ permutations of the corresponding binary strips. We refer to this binary ensemble as \mathcal{B} .

The distance properties of these two binary ensembles are different, and the choice of ensemble depends on the mapping performed by the PAM modulator. In what follows, we analyze the ensemble \mathcal{N} in relation to SICM mapping, and the binary ensemble \mathcal{B} to analyzing NB LDPC codes used with BICM. In the next subsections, we present a technique for computing the average SEDS for the ensembles \mathcal{N} and \mathcal{B} used with PAM signaling.

B. Average squared Euclidean distance spectrum of the ensemble of NB LDPC coded PAM signals

In order to compute bound (25) for the aforementioned NB LDPC code ensemble used in conjunction with PAM signaling, it is necessary to know its SEDS. There are two obstacles related to the computing of the SEDS of the coded modulation signals. First, the spectrum depends on the indexing of the signal points and the symbol-to-PAM-signal mapping. Second, despite the code linearity in the Hamming space, the corresponding set of the coded modulation signal sequences does not form a linear subspace of the Euclidean space. Consequently, the modulated codewords can have different decoding error probabilities.

The first obstacle can be overcome by deriving the SEDS via the average symbol (bit) Hamming weight spectrum for the ensemble \mathcal{N} and for its binary image \mathcal{B} in the cases of SICM and BICM, respectively. The second obstacle we overcome by following the approach [28]. More specifically, for a chosen code symbol-to-PAM-signal mapping, averaging of the ensemble average SEDS is performed over the pairs of codewords of a given code in the ensemble.

In the calculations below, we use notions of combinatorial and moment generating functions as well as the composition of generating functions. For completeness of the paper, the corresponding definitions and lemma are given in Appendix.

Summarizing, we aim at deriving the average SEDS for the ensemble \mathcal{N} and its binary image \mathcal{B} . They are obtained in two steps. First, the average Hamming spectra for these ensembles are derived. Then compositions of the derived averaged Hamming weight generating functions with the moment generating function of the normalized squared Euclidean distance (SED) between PAM signals per symbol Hamming weight or bit, are computed.

Next, we revise the approach to calculating the precise average symbol and bit Hamming weight enumerators of the ensemble of NB LDPC codes.

1) *Average Hamming weight spectra for the ensembles \mathcal{N} and \mathcal{B} :* The average combinatorial generating function (CGF) $F(s)$ for the q -ary symbol Hamming weight enumerator of the ensemble \mathcal{N} is derived in [13]. It has the form

$$F(s) = \sum_{w=0}^N F_{N,w} s^w, \quad (9)$$

$$F_{N,w} = (q-1)^{w(1-J)} \binom{N}{w}^{1-J} \prod_{j=1}^J f_{j,w}^{\text{strip}},$$

where, as shown in [13], the symbol Hamming weight enumerator CGF for the sequences \mathbf{x} satisfying the j -th strip of the parity-check matrix is

$$f_j^{\text{strip}}(s) = \sum_{w=0}^N f_{j,w}^{\text{strip}} s^w = (f_j^{\text{row}}(s))^L, \quad j = 1, \dots, J \quad (10)$$

and

$$f_j^{\text{row}}(s) = \sum_{w=0}^{K_j} f_{j,w}^{\text{row}} = \frac{(1 + (q-1)s)^{K_j} + (q-1)(1-s)^{K_j}}{q} (1 + (q-1)s)^{K-K_j}$$

is the weight enumerator CGF of q -ary sequences \mathbf{x} of length $N = n/m$ satisfying the nonzero part of one q -ary parity-check equation, $f_{j,w}^{\text{strip}}$ is the w -th coefficient of the series expansion for $f_j^{\text{strip}}(s)$.

In order to derive the average CGF $\Psi(\rho)$ for the ensemble \mathcal{B} , we compute the CGF for the number of binary sequences satisfying a system of parity-check equations of a binary strip of size $Lm \times n$ in the binary image of the parity-check matrix as composition of generating functions

$$\psi_i^{\text{strip}}(\rho) = (f_i^{\text{row}}(s))^L \Big|_{s=\phi(\rho)} = (f_i^{\text{row}}(\phi(\rho)))^L, \quad i = 1, \dots, J, \quad (11)$$

where $i = 1, 2, \dots, J$, and $\phi(\rho)$ as in [36], [35], denotes the moment generating function (MGF) of the nonzero $q = 2^m$ -ary symbol values

$$\phi(\rho) = \sum_{i=1}^m \frac{1}{q-1} \binom{m}{i} \rho^i = \frac{(1+\rho)^m - 1}{q-1}. \quad (12)$$

Similarly to (9), the average CGF of the binary ensemble \mathcal{B} is

$$\Psi(\rho) = \sum_{w=0}^n \Psi_w \rho^w; \quad \Psi_w = \binom{n}{w}^{1-J} \prod_{j=1}^J \psi_{j,w}^{\text{strip}}, \quad (13)$$

where $\psi_{j,w}^{\text{strip}}$ is the w -th coefficient of series expansion for $\psi_j^{\text{strip}}(\rho)$.

It is easy to see that computing the finite-length average symbol (bit) Hamming weight spectrum for NB LDPC codes is reduced to computing coefficients of series expansion for functions f_j^{strip} in (10) and $\psi_j^{\text{strip}}(\rho)$ in (11), $j = 1, 2, \dots, J$. It can be done recursively as in [35]. Numerical problems can be overcome by performing computations in logarithmic domain.

2) *Average squared Euclidean distance spectra of the ensembles \mathcal{N} and \mathcal{B}* : Next, we derive the average SEDS in terms of the known functions $\tilde{F}(s)$ or $\Psi(\rho)$ depending on the mapping used.

Assume that an p -bit binary sequence is associated with each PAM signal point in the set $\{-2^p + 1, \dots, -1, 1, \dots, 2^p - 1\}$, for example, as in Table II. Similarly to the approach in [36] and [35], we use Lemma 1 in order to represent the CGF of the average SEDS $A^{\text{symb}}(\lambda)$ and $A^{\text{bit}}(\lambda)$ for the ensembles \mathcal{N} and \mathcal{B} as a composition of the CGF $\tilde{F}(s)$ and $\Psi(\rho)$, respectively, with the MGF of the normalized SED between the PAM signal points.

We start with considering bit-to-PAM signal based mappings: BICM, BPCM, and ASCM. When BICM is used, each group of p sequential bits are mapped onto one of 2^p -PAM signals. In the case of multi-signal mappings such as BPCM and ASCM, we consider groups of n_s sequential $q = 2^m$ -ary symbols, that is, groups of $n_s m$ bits mapped onto the group of n_p 2^p -PAM signals, where

$$n_s m = n_p p = n, \quad (14)$$

and n_s, n_p are the smallest integers satisfying (14). Denote by $\mathbf{s} = (s_1, \dots, s_{n_p})$ a vector of n_p 2^p -PAM signals. Then we compute SEDs $d_{\text{E}}^2(\mathbf{s}_i, \mathbf{s}_j)$ for all possible vector pairs $\mathbf{s}_i, \mathbf{s}_j$, and Hamming distance $d_{\text{H}}(\mathbf{s}_i, \mathbf{s}_j)$ between the binary representations of \mathbf{s}_i and \mathbf{s}_j .

TABLE III: $d_H(\mathbf{s}_i, \mathbf{s}_j)/(d_E^2(\mathbf{s}_i, \mathbf{s}_j))$ for pairs of 4-PAM signals

$\mathbf{s}_i/\mathbf{s}_j$	00(-3)	01(-1)	11(1)	10(3)
00(-3)	0(0)	1(4)	2(16)	1(36)
01(-1)	1(4)	0(0)	1(4)	2(16)
11(1)	2(16)	1(4)	0(0)	1(4)
10(3)	1(36)	2(16)	1(4)	0(0)

TABLE IV: $d_H(\mathbf{s}_i, \mathbf{s}_j)/(d_E^2(\mathbf{s}_i, \mathbf{s}_j))$ for pairs of 8-PAM signals

$\mathbf{s}_i/\mathbf{s}_j$	000(-7)	001(-5)	011(-3)	010(-1)	110(1)	111(3)	101(5)	100(7)
000(-7)	0(0)	1(4)	2(16)	1(36)	2(64)	3(100)	2(144)	1(196)
001(-5)	1(4)	0(0)	1(4)	2(16)	3(36)	2(64)	1(100)	2(144)
011(-3)	2(16)	1(4)	0(0)	1(4)	2(16)	1(36)	2(64)	3(100)
010(-1)	1(36)	2(16)	1(4)	0(0)	1(4)	2(16)	3(36)	2(64)
110(1)	2(64)	3(36)	2(16)	1(4)	0(0)	1(4)	2(16)	1(36)
111(3)	3(100)	2(64)	1(36)	2(16)	1(4)	0(0)	1(4)	2(16)
101(5)	2(144)	1(100)	2(64)	3(36)	2(16)	1(4)	0(0)	1(4)
100(7)	1(196)	2(144)	3(100)	2(64)	1(36)	2(16)	1(4)	0(0)

Consider a set of pairs of NB LDPC coded sequences of 2^p -PAM signals with one of the bit-to-PAM signal mappings corresponding to pairs of codewords $\mathbf{v}_i, \mathbf{v}_j$ of length n bits at Hamming distance d . We introduce the average over this set MGF of the SEDs between signal groups normalized per the corresponding Hamming distance

$$\alpha_{n,d}(\lambda) = \sum_{i=1}^{M^{np}} \sum_{j \neq i} \Pr \{d_E^2(\mathbf{s}_i, \mathbf{s}_j), d_H(\mathbf{s}_i, \mathbf{s}_j) | n, d\} \lambda^{\delta_{ij}}, \quad (15)$$

where

$$\delta_{ij} = \frac{d_E^2(\mathbf{s}_i, \mathbf{s}_j)}{d_H(\mathbf{s}_i, \mathbf{s}_j)},$$

is the normalized SED between PAM signal points at the SED $d_E^2(\mathbf{s}_i, \mathbf{s}_j)$ and the Hamming distance $d_H(\mathbf{s}_i, \mathbf{s}_j)$ between their binary representations.

For 4-PAM and 8-PAM signaling used with BICM mapping, the δ_{ij} values are given in Table III and IV, respectively.

For a given Hamming distance $d_H(\mathbf{s}_i, \mathbf{s}_j)$ the corresponding value of SED is a random variable which does not depend on n, d . Therefore, (15) can be expressed as

$$\alpha_{n,d}(\lambda) = \sum_{d_H} \Pr(d_H(\mathbf{s}_i, \mathbf{s}_j) | n, d) \sum_{j \neq i} \Pr(d_E^2(\mathbf{s}_i, \mathbf{s}_j) | d_H(\mathbf{s}_i, \mathbf{s}_j)) \lambda^{\delta_{ij}}. \quad (16)$$

Let us denote $\Pr(d_H(\mathbf{s}_i, \mathbf{s}_j) | n, d)$ by $\{p_{n,d}(\tau)\}$, where $\tau = d_H(\mathbf{s}_i, \mathbf{s}_j)$. Then, for 4-PAM signaling with BICM and with the Gray indexing, from Table III we obtain the MGF:

$$\alpha_{n,d}(\lambda) = p_{n,d}(1) \frac{1}{4} (3\lambda^4 + \lambda^{36}) + p_{n,d}(2) \lambda^8. \quad (17)$$

Similarly, for 8-PAM signaling with the Gray mapping as in Table II, we have from Table IV

$$\begin{aligned} \alpha_{n,d}(\lambda) &= p_{n,d}(1) \frac{1}{12} (7\lambda^4 + 3\lambda^{36} + \lambda^{100} + \lambda^{196}) \\ &+ p_{n,d}(2) \frac{1}{6} (3\lambda^8 + 2\lambda^{32} + \lambda^{72}) \\ &+ p_{n,d}(3) \frac{1}{2} (\lambda^{12} + \lambda^{100/3}). \end{aligned} \quad (18)$$

From (17) and (18) we see that the polynomials $\alpha_{n,d}(\lambda)$ are sparse. For a particular mapping it is convenient to represent them by two matrices: the matrix of probabilities and the matrix of degrees. Collection of polynomials for BICM, BPCM, and ASCM mappings used with 4-PAM and 8-PAM signaling is tabulated in Table V of Appendix C.

In order to compute $\alpha_{n,d}(\lambda)$, we have to find the probability distributions $p_{n,d}(\cdot)$ for the number of ones in the binary representations of PAM signals. The simplest assumption is that d nonzero bits are uniformly distributed over n code bits and that

$$p_{n,d}(\tau) = \binom{n_s m}{\tau} \left(\frac{d}{n}\right)^\tau \left(\frac{n-d}{n}\right)^{n_s m - \tau}.$$

Tighter and more complex assumption takes into account that the sum of block weights τ is equal to d and these weights are dependent, that is,

$$p_{n,d}(\tau) = \frac{\binom{n_s m}{\tau} \binom{n - n_s m}{d - \tau}}{\binom{n}{d}}.$$

Under condition $p \ll n$ these two approaches give the same result.

The analysis of the SICM mapping is based on the MGF of the normalized pairwise SEDs between signal points computed under assumption of the uniform distribution of the binary indices of the $M = 2^p$ -ary PAM signal points. It has the form

$$\alpha(\lambda) = \frac{1}{M(M-1)} \sum_{i=1}^M \sum_{j \neq i} \lambda^{\delta_{ij}}.$$

For example, for 4-PAM signaling with SICM with the Gray indexing, from Table III we obtain the MGF:

$$\alpha(\lambda) = \frac{1}{6} (3\lambda^4 + 2\lambda^8 + \lambda^{36}). \quad (19)$$

Similarly, for 8-PAM signaling with the Gray mapping as in Table II, we have

$$\alpha(\lambda) = \frac{1}{28} (7\lambda^4 + 6\lambda^8 + 2\lambda^{12} + 4\lambda^{32} + 3\lambda^{36} + 2\lambda^{100/3} + 2\lambda^{72} + \lambda^{100} + \lambda^{189}). \quad (20)$$

In order to simplify the analysis of nonlinear subspaces of coded modulation signal sequences, we introduce *the cumulative normalized SED* between two sequences $\mathbf{s}_l = (s_{l1}, \dots, s_{lN_p})$ and $\mathbf{s}_t = (s_{t1}, \dots, s_{tN_p})$ of PAM signal points corresponding to a pair of codewords $\mathbf{c}_l = (c_{l1}, \dots, c_{lN})$, $\mathbf{c}_t = (c_{t1}, \dots, c_{tN})$ at the Hamming distance $d_H(\mathbf{c}_l, \mathbf{c}_t) = d$. It is defined as

$$\Delta(\mathbf{c}_l, \mathbf{c}_t) = \sum_{i \in \mathcal{D}_{lt}} \gamma_i, \quad \gamma_i = \frac{d_E^2(s_{li}, s_{ti})}{d_H(c_{li}, c_{ti})}, \quad \gamma_i = 0 \text{ if } c_{li} = c_{ti}, \quad (21)$$

where \mathcal{D}_{lt} is a set of non-coinciding bit positions in \mathbf{c}_l and \mathbf{c}_t .¹ The key point here is that we ignore the fact that the bits in different positions make a different contribution to the SED. The reason for neglecting this fact is that we consider the average contribution of bits in different positions, where averaging is performed over pairs of codewords at a given distance d under a fixed mapping.

For codewords \mathbf{v}_i and \mathbf{v}_j at Hamming distance d by considering $\Delta(\cdot, \cdot)$ as a sum of d i.i.d. variables γ_i we obtain from (21) MGF for the cumulative normalized SEDs between the coded modulation sequences corresponding to \mathbf{v}_i and \mathbf{v}_j as

$$G_d(\lambda) = \alpha_{n,d}^d(\lambda),$$

¹The cumulative normalized SED is an approximation of the normalized SED between signal sequences. It is used in order to apply composition of generating functions for the analysis. Although (21) is not applicable for fixed codes and fixed mappings but gives a valid approximation on average over the product ensemble of random codes and random mappings.

where $\alpha_{n,d}(\lambda)$ is defined in (16) and exemplified in (17) and (18).

For the ensemble \mathcal{B} , spectrum of pairwise Hamming distances is determined by GF $\Psi(\rho)$ (13). Therefore, under assumption (21) the corresponding SEDS is also determined by $\Psi(\rho)$. By composing (13) and $G_d(\lambda)$ we derive the CGF of the average SEDS for BICM, ASICM, and BPCM mappings in the form

$$\begin{aligned} A_n(\lambda) &= \sum_{\Delta} A_n(\Delta) \lambda^{\Delta} = \sum_{\Delta} \sum_w A_n(w, \Delta) \lambda^{\Delta} \\ &= \sum_w \Psi_w \sum_{\Delta} \frac{A_n(w, \Delta)}{\Psi_w} \lambda^{\Delta} \\ &= \sum_w \Psi_w \sum_{\Delta} P_w(\Delta) \lambda^{\Delta} = \sum_w \Psi_w G_w(\lambda), \end{aligned} \quad (22)$$

where $A_n(w, \Delta)$ is the average number of codeword pairs at Hamming distance w and at the cumulative normalized SED Δ , $P_w(\Delta) = A_n(w, \Delta)/\Psi_w$ is a probability distribution on cumulative distance Δ for a given w .

When SICM mapping is used, we first derive the composition of the $q = 2^m$ -ary weight CGF F for the ensemble \mathcal{N} and the MGF of the q -ary nonzero symbol represented in the form of m/p PAM signals

$$\theta(s) = \frac{(1 + (M-1)s)^{m/p} + (M-1)(1-s)^{m/p}}{q-1}. \quad (23)$$

By applying Lemma 1 in Appendix B, in the case of SICM mapping we obtain the CGF for the normalized cumulative SEDS as

$$A(\lambda) = F(\theta(s)) = F(\theta(\alpha(\lambda))). \quad (24)$$

In Figs. 2, 3 the average SEDS for the ensembles of NB LDPC codes over $\text{GF}(2^4)$ and $\text{GF}(2^6)$ used with the 4-PAM signaling are shown for the cases $w = 2.25$ and $w = 2.83$, where w denotes the average column weight of the base parity-check matrix. For comparison, the average SEDS for the ensembles of general random binary and general random NB codes over the same fields are presented in the same figures. Notice, that the average Hamming weight spectrum coefficients for the rate $R = (N-r)/N$ q -ary linear code of length N are

$$F_{N,w} = 2^{-r} \binom{N}{w} (q-1)^w.$$

If $q = 2$, we obtain the average Hamming weight spectrum coefficients for the binary random code of the same rate and length. It follows from the presented plots that SICM provides better SEDS than BICM independently of the value of m . As expected, the SEDS of the NB LDPC codes from the ensemble are approaching the SEDS of general random NB codes when w grows.

In Fig. 4, we present the average SEDS for the ensemble of NB LDPC codes with $w \in \{2.25; 2.5; 2.83\}$ over $\text{GF}(2^4)$ used with 8-PAM signaling. The average SEDS for ASCM mapping are compared to the average SEDS for BICM mapping used with the same code ensembles. In the same figure, the average SEDS for the general binary random code used with 8-PAM signaling and BICM mapping is shown. It follows from the presented results, that ASCM SEDS are better than the corresponding BICM spectra.

In the next section, we present the random coding bound on the ML decoding error probability obtained by substituting spectra (22) and (24) to the HP upper bound (25).

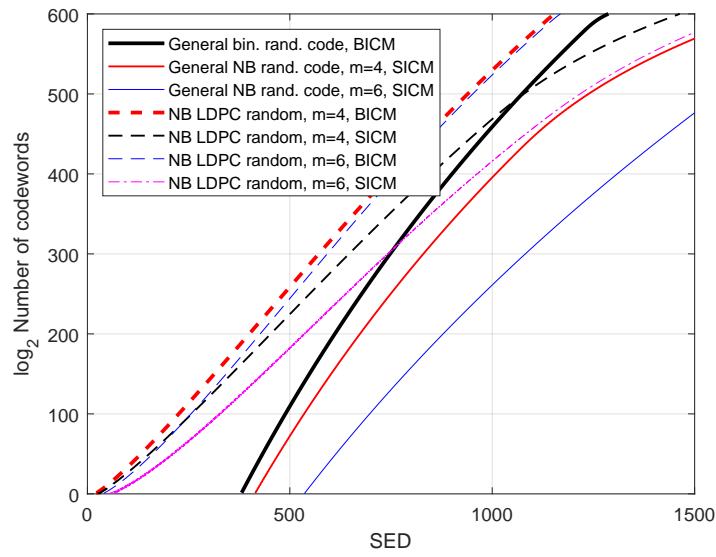


Fig. 2: Average cumulative normalized SED spectrum for the ensemble of NB LDPC codes over $GF(2^4)$ and $GF(2^6)$ used with 4-PAM signaling and different mappings. The average column weight of the base matrix is $w = 2.25$

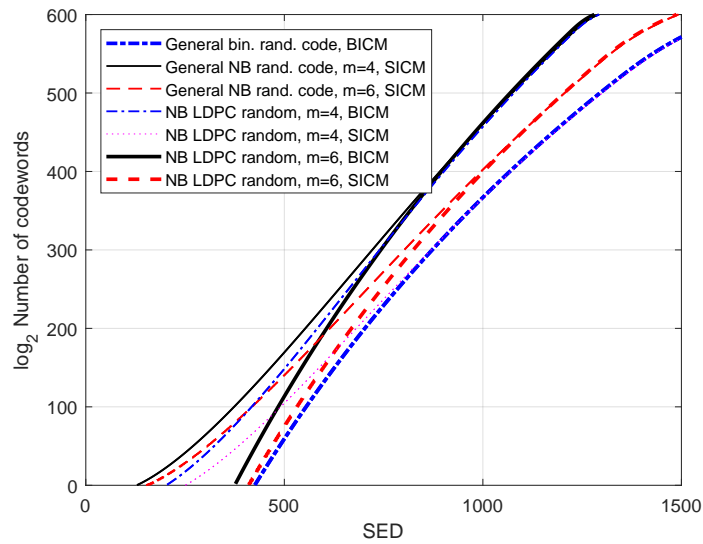


Fig. 3: Average cumulative normalized SED spectrum for the ensemble of NB LDPC codes over $GF(2^4)$ and $GF(2^6)$ of the base matrix used with 4-PAM signaling and different mappings. The average column weight of the base matrix is $w = 2.83$

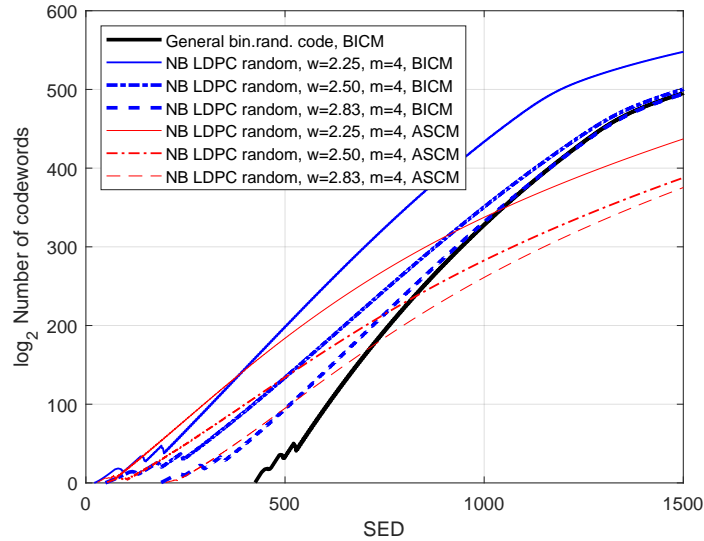


Fig. 4: Average cumulative normalized SED spectrum for the ensemble of NB LDPC codes over $\text{GF}(2^4)$ of the base matrix used with 8-PAM signaling and BICM and ASCM mappings.

V. NUMERICAL RESULTS

In this section, first, we compute the random coding bounds on the ML decoding error probability for the ensemble of NB LDPC codes over $\text{GF}(2^4)$ and $\text{GF}(2^6)$ used with 4-PAM and 8-PAM signaling and different mappings. These bounds are obtained by substituting the average spectra (22) and (24) into the HP upper bound (25). Comparison of these bounds with the bound (25) calculated for the general binary random linear code and the general NB random linear code of the same length is performed. Then we present the simulation results for the FER performance of BP decoding for the NB QC-LDPC codes over $\text{GF}(2^4)$ and $\text{GF}(2^6)$, optimized as in [13] and [15]. We compare the FER performance of BP decoding with the random coding bound on ML decoding error probability for random almost regular NB LDPC codes of the same length and alphabet sizes.

In the sequel, we use notation SNR for signal-to-noise ratio per signal component measured in dB, w denotes the average column weight, J and K denote the maximal number of nonzero elements in each column and each row of the parity-check matrix, respectively.

A. Calculation of random coding bounds

We analyze the ensemble of random almost regular rate $R = 3/4$ NB LDPC codes determined by the base matrix of size 3×12 . In all examples, parity-check matrices have row weights $K_1 \leq K, K_2 = K_3 = K$. The average column weight is computed as $w = (24 + K_1)/12$.

The bounds on the error probability of ML decoding for NB random LDPC codes as well as the general binary and NB random linear codes are plotted in Figs. 5 – 8 for different alphabet sizes and modulation orders. For comparison in the same figures, we plotted the FER performance of NB QC-LDPC codes of the same length and alphabet size.

The presented bounds show that

- ML decoding error probability bounds for different parameters of the NB LDPC code ensemble and different mappings demonstrate the advantage of SICM and ASCM mappings over the BICM mapping. The presented bounds show error floor phenomena for some scenarios and demonstrate

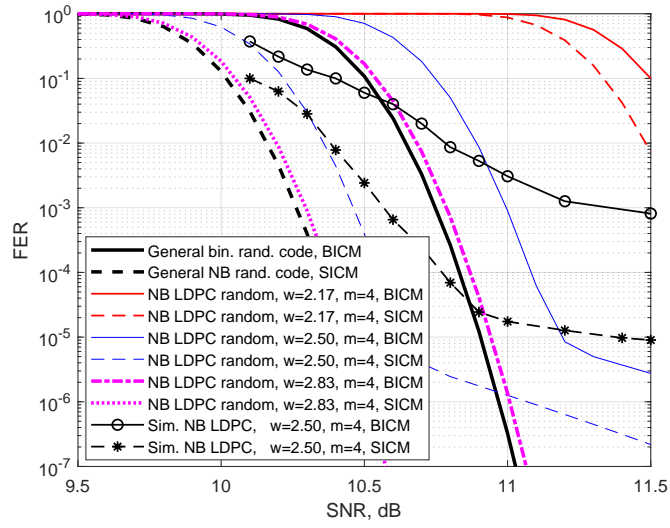


Fig. 5: Bounds on the error probability of the ML decoding for rate $R = 3/4$ NB LDPC codes over $GF(2^4)$ of length about 2000 bits with 4-PAM signaling. BICM limit is equal to 9.304 dB.

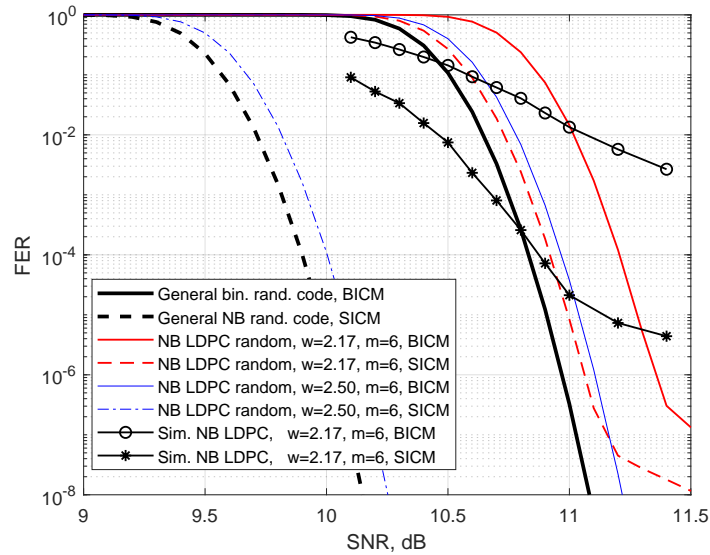


Fig. 6: Bounds on the error probability of the ML decoding for rate $R = 3/4$ NB LDPC codes over $GF(2^6)$ of length about 2000 bits with 4-PAM signaling. BICM limit is equal to 9.304 dB.

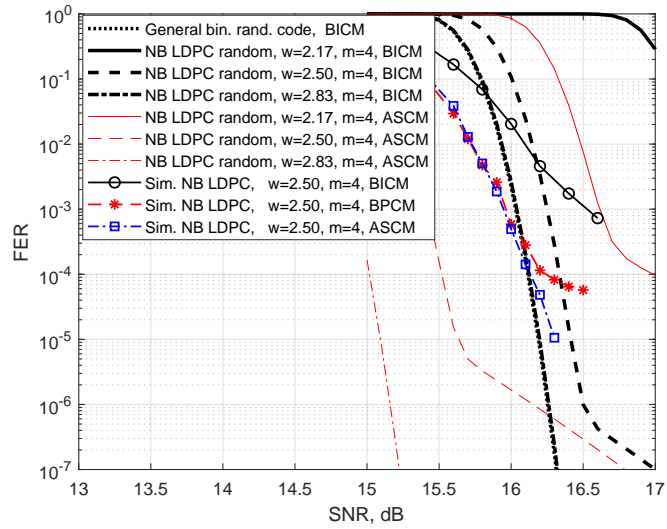


Fig. 7: Bounds on the error probability of the ML decoding for rate $R = 3/4$ NB LDPC codes over $GF(2^4)$ of length about 2000 bits with 8-PAM signaling. BICM limit is equal to 14.365 dB.

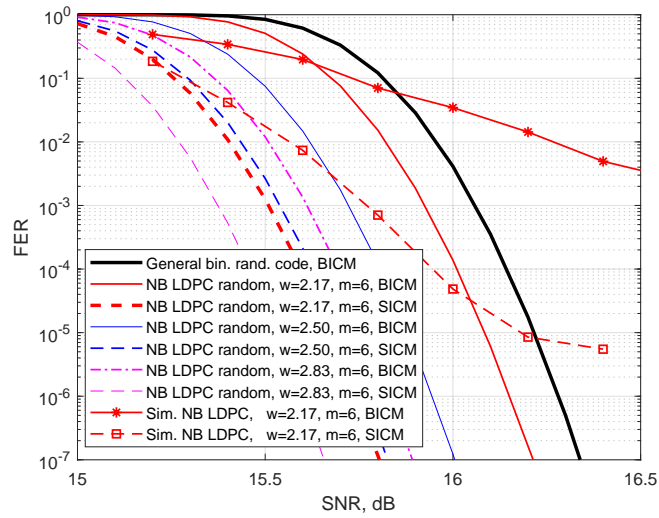


Fig. 8: Bounds on the error probability of the ML decoding for rate $R = 3/4$ NB LDPC codes over $GF(2^6)$ of length about 2000 bits with 8-PAM signaling. BICM limit is equal to 14.365 dB.

performance behavior depending on the average column weight w . The predicted behavior matches the simulated results for the NB QC-LDPC codes with the same alphabet size and the same average column weight w , although, numerically the simulation results for the BP decoding performance differ from the predicted ML decoding performance. Thus, the approach based on the normalized SEDS can be considered as a useful technique for the analysis of practical coded modulation systems.

- Unlike the FER performance of general binary and NB random linear codes, the FER performance of NB LDPC codes over $\text{GF}(2^4)$ and $\text{GF}(2^6)$ used with both 4-PAM and 8-PAM signaling have severe error floors independently on the used mapping. Increase in the average column weight w lowers the error floor level.
- Both the bounds and the simulation results suggest that in the waterfall region, the FER performance of the NB LDPC codes used with BICM is significantly worse than the FER performance of NB LDPC codes with SICM independently of the alphabet size and modulation order. Reduction in the average column weight w monotonically worsens the FER performance of the ML decoding.
- For the sets of coded modulation system parameters where SICM mapping cannot be applied, ASCM and BPCM mappings provide the ML decoding performance which is superior to the case when BICM mapping is used.
- Random coding bounds for ASCM and BPCM used in the 8-PAM scenario with $m = 4$ numerically coincide with each other (see Appendix C). However, when used with BP decoding, ASICM provides slightly better results than BPCM.
- When increasing m and w , NB random LDPC codes used with BICM and SICM provide the ML decoding FER performance rather close to that of the binary random linear and NB random linear codes, respectively.

B. NB QC-LDPC codes with QAM signaling

It is well known that due to their structural properties, QC-LDPC codes are widely used in modern communication standards such as WiFi, WiMAX, DVB-S2, and 5G standards. In this subsection, we present simulation results of the BP decoding for moderate length (about 2000 bits) optimized NB QC-LDPC codes used with PAM signaling and different mappings. Comparison with the derived bounds as well as with the BP decoding performance for best known binary and NB LDPC codes with the same parameters are performed.

It is expected that sparser codes are weaker in the sense of ML decoding performance. However, sparseness is important for improving the performance of BP decoding. The goal of our computations and simulations is to evaluate a sparsity factor which allows to stay close to optimal codes in the sense of ML decoding and to improve as much as possible BP decoding performance.

In the following, we consider a set of rate $R = 3/4$ NB QC-LDPC codes with maximum column weight of their parity-check matrices $J = 3$ optimized by using techniques in [13] and [15]. NB QC-LDPC codes of length about 2000 bits with different average column weight w of their base parity-check matrices are studied. All considered NB QC-LDPC codes are determined by the base matrix of size 14×56 with column weights two and three, the lifting factor L is chosen to be equal to 9, 8, and 6 for the code over $\text{GF}(2^4)$, $\text{GF}(2^5)$, and $\text{GF}(2^6)$, respectively. The average column weight w takes on values from the set $\{2.17, 2.27, 2.35, 2.50, 2.67, 2.71\}$. These codes used with 4-PAM and 8-PAM signaling were simulated over the AWGN channel. The FER performance of sum-product BP decoding was simulated with a maximum of 100 iterations until 50 block errors.

The obtained FER performance of the BP decoding when using different demodulators for the field extension order $m = 4$, $m = 5$, and $m = 6$, respectively, and for the 4-PAM signaling is shown in Figs. 9 – 11. Comparison with the standard binary code in the WiFi standard as well as with the binary code in 5G standard is made. In the same figures we showed the ML decoding error probability bound

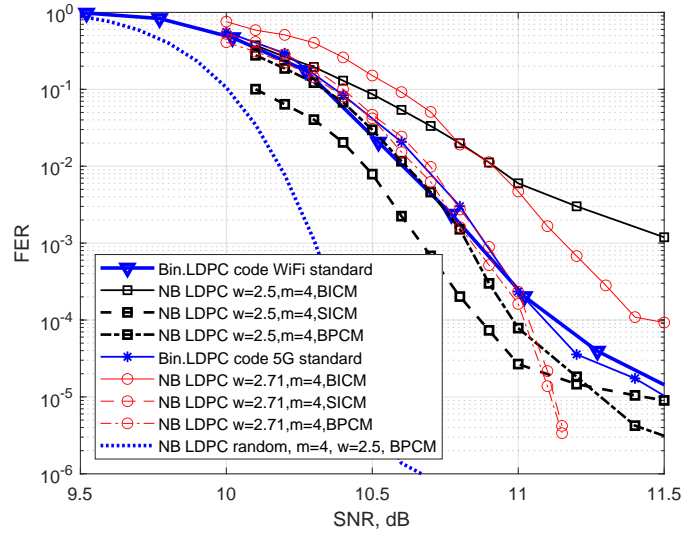


Fig. 9: FER performance of the BP decoding for rate $R = 3/4$ NB QC LDPC codes of length 2016 bits over $\text{GF}(2^4)$ with 4-PAM signaling. BICM limit is equal to 9.304 dB.

for the NB random LDPC code with parameters m and w which provide the best FER performance of the sum-product decoding. All figures are accompanied by a value of the BICM limit.

It is easy to notice that the FER performance of the BP decoding for NB QC-LDPC codes in a large degree depends on the chosen mapping. The NB QC-LDPC codes used with BICM show the FER performance, which is inferior to the corresponding performance of the binary codes. Both SICM and BPCM mappings provide a gain of about 0.5 dB with respect to the binary case. Increasing the number of weight three columns in the base matrix of the considered NB QC-LDPC codes, as expected, improves the FER performance of BP decoding in the error floor region but worsens the FER performance at low SNRs independently on the mapping used. In Fig. 10, the FER performances of two NB QC-LDPC codes ($w = 2.35$ and $w = 2.71$) used with 4-PAM and BICM are shown. The NB QC-LDPC code with $w = 2.71$ outperforms the NB QC-LDPC code with $w = 2.35$ in the error floor region but loses at low SNRs. It follows from the presented plots that the ML decoding error probability bound mimics the behavior of the BP decoding FER performance. The observed gap between the bound and the simulation results is about 0.2–0.5 dB at the $\text{FER} \approx 10^{-4}$.

Simulation results for NB QC-LDPC codes with 8-PAM signaling and field extensions $m = 4$ and $m = 6$ are presented in Figs. 12–13. Similarly to the 4-PAM case, NB QC-LDPC codes with BICM exhibit FER performance which is inferior to that of the binary code. NB QC-LDPC codes with SICM and ASCM demonstrate a 0.5 dB gain over the binary code. Comparison of the performance curves for the NB codes over $\text{GF}(2^6)$ with $w = 2.17$ and $w = 2.27$ in Fig. 13 shows that increasing the number of weight three columns in the code base matrix if 8-PAM signaling is used with BICM does not improve performance significantly.

Notice that the obtained results are consistent with conclusions drawn in [6] and [12] for regular NB LDPC codes. In particular, BICM used with both 4-PAM and 8-PAM signaling loses about 1 dB compared to SICM used with the same signaling. Comparison with the bound shows a gap of 0.1–0.6 dB at the $\text{FER} \approx 10^{-4}$.

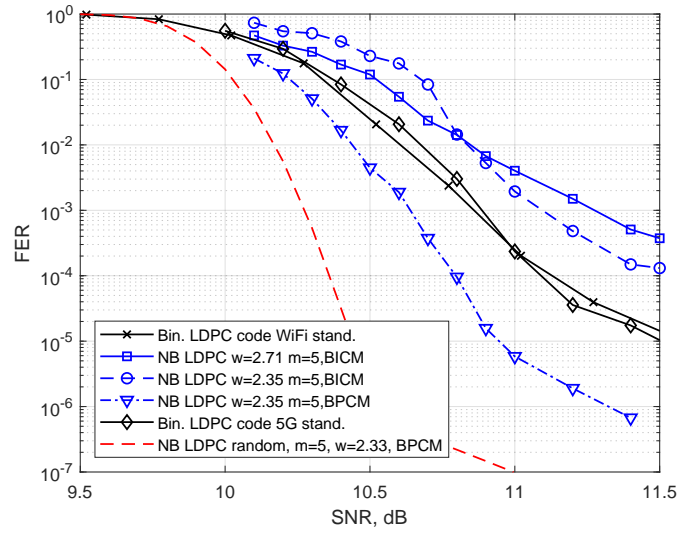


Fig. 10: FER performance of the BP decoding for rate $R = 3/4$ NB QC LDPC codes of length 2240 bits over $GF(2^5)$ with 4-PAM signaling. BICM limit is equal to 9.304 dB.

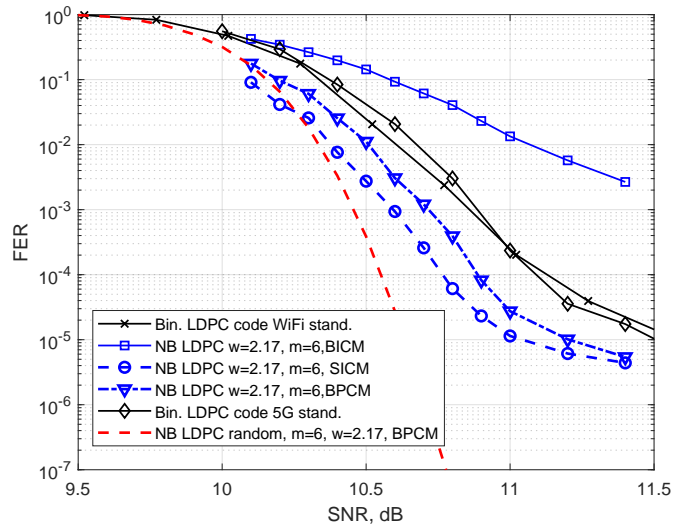


Fig. 11: FER performance of the BP decoding for rate $R = 3/4$ NB QC LDPC codes of length 2016 bits over $GF(2^6)$ with 4-PAM signaling. BICM limit is equal to 9.304 dB.

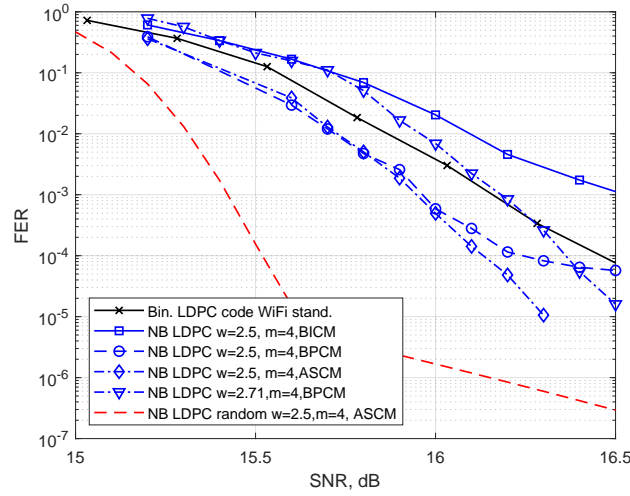


Fig. 12: FER performance of the BP decoding for rate $R = 3/4$ NB QC LDPC codes of length 2016 bits over $GF(2^4)$ with 8-PAM signaling. BICM limit is equal to 14.365 dB.

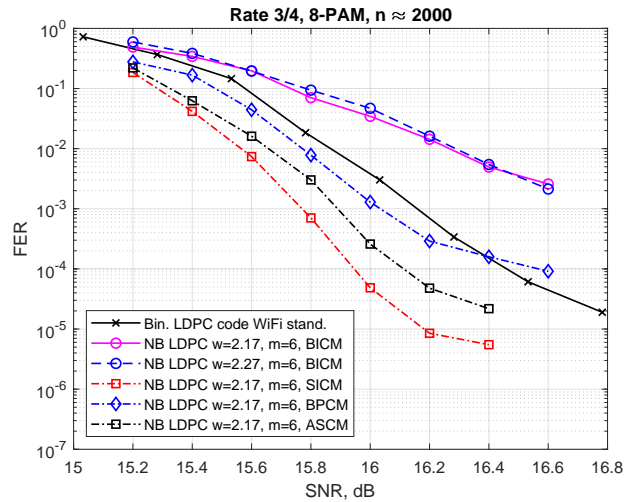


Fig. 13: FER performance of the BP decoding for rate $R = 3/4$ NB QC LDPC codes of length 2016 bits over $GF(2^6)$ with 8-PAM signaling. BICM limit is equal to 14.365 dB.

VI. CONCLUSION

NB QC-LDPC codes used with QAM signaling over the AWGN channel were analyzed. Four different mappings of code symbols to QAM signals were studied. It was shown that BICM used with both 4-PAM and 8-PAM signaling is inferior to SICM with the same signaling by about 1 dB.

The NB QC-LDPC codes used in conjunction with BICM exhibit the FER performance which is inferior to that of the binary counterparts. More sophisticated mappings could provide for better performance compared to the BICM. If the modulation order is not a divisor of the alphabet order, then the BPCM and ASCM outperform the BICM by about 0.5 dB. Yet, these mappings do not improve

the performance with respect to SICM when the modulation order is not a divisor of the alphabet order.

The random ensemble of almost regular NB LDPC codes used with QAM signaling was analyzed. The average squared Euclidean distance spectra for codes in this ensemble used with different mappings were derived. By substituting the computed average squared Euclidean distance spectra to the Herzberg-Poltyrev upper bound, the tightened finite-length upper bounds on the error probability of ML decoding for irregular NB LDPC codes over $\text{GF}(2^m)$ were derived. The obtained random coding bound mimics the behavior of the FER performance of BP decoding of practical NB QC-LDPC codes. In particular, in some scenarios it exhibits a severe error floor independently of the mapping used. The gap between the bound and the simulation results varies from 0.1 to 0.6 dB depending on the alphabet size, code density, and modulation order. The presented simulation results and comparisons with the bounds on error probability showed that NB QC-LDPC codes outperform known binary QC-LDPC codes.

APPENDIX

A. Upper bound

The Shannon-Herzberg-Poltyrev [28] is valid for arbitrary signal sets of length n signals

$$P_e \leq \sum_{w \leq w_0} S_w \Theta_w(x) + 1 - \chi_{n-1}^2 \left(\frac{w_0}{\sigma^2} \right). \quad (25)$$

Here

$$\Theta_w(x) = \int_{\sqrt{w}/2}^{\sqrt{w_0}} f \left(\frac{y}{\sigma} \right) \phi_{n-1} \left(\frac{w_0 - y^2}{\sigma^2} \right) dy$$

and

$$\begin{aligned} f(x) &= \frac{1}{\sqrt{2\pi}} \exp \left\{ -\frac{x^2}{2} \right\}, \\ \phi_n(x) &= \frac{x^{n/2-1} e^{-x/2}}{2^{n/2} \Gamma(n/2)}, \\ \chi_n^2(x) &= \frac{\gamma(n/2, x/2)}{\Gamma(n/2)} \end{aligned}$$

are Gaussian probability density function, probability density function and probability distribution function of the χ -squared distribution with n degrees of freedom, respectively, S_w is the w -th spectrum coefficient, and parameter w_0 is a solution of the equation

$$\sum_{w \leq w_0} S_w \int_0^{\arccos \sqrt{\frac{w}{4w_0}}} \sin^{n-3} \phi \, d\phi = \sqrt{\pi} \frac{\Gamma(\frac{n-2}{2})}{\Gamma(\frac{n-1}{2})}. \quad (26)$$

B. Generating functions. Compositions of generating functions

The *combinatorial generating function* (CGF) $\psi(s)$ for a sequence of nonnegative numbers u_0, u_1, \dots is defined as

$$\psi(s) = \sum_{i=0}^{\infty} u_i s^i,$$

where s is a formal variable. We interpret u_i as a multiplicity of occurrences of value i in the same realization. If the sequence \mathbf{u} is random then the *average combinatorial generating function* $\tilde{\psi}(s)$ of \mathbf{u} is obtained by averaging $\psi(s)$ over all possible vectors \mathbf{u} .

The *moment generating function* (MGF) $\theta(\rho)$ for a discrete random variable $v \in V$ is defined as

$$\theta(\rho) = \sum_{v \in V} p(v) \rho^v,$$

where $p(v)$ is the probability of v , $\sum_{v \in V} p(v) = 1$ and ρ is a formal variable.

Let $f(s) = \sum f_n s^n$ and $g(s) = \sum g_n s^n$ be generating functions, then *composition of generating functions* $f(s)$ and $g(s)$ is defined as $\sum_{n=0}^{\infty} f_n (g(s))^n$.

Lemma 1: Let a non-random sequence $\mathbf{u} = (u_0, u_1, \dots)$, $u_i \geq 0$ have CGF $\psi(s)$ and $\mathbf{v} = (v_0, v_1, \dots)$ be a sequence of independent identically distributed discrete random variables $v_i \in V$ having MGF $\theta(\rho)$ each. Introduce a new random variable

$$z_j = \sum_{i=0}^{u_j} v_i, \quad j = 0, 1, \dots \quad (27)$$

Then the average over all possible \mathbf{v} CGF $\Psi(\rho)$ of the sequence $\mathbf{z} = (z_0, z_1, \dots)$ is equal to

$$\Psi(\rho) = \psi(s)|_{s=\theta(\rho)} = \psi(\theta(\rho)). \quad (28)$$

Proof: This lemma is a straightforward generalization of formula (1.3) [37, Chapter XII]. ■

C. Examples of SEDS for BICM, BPCM and ASCM mapping

Examples of MGF of normalized SEDS $\alpha_{n,d}$ computed by using (16) are given in Table V. Each $\alpha_{n,d}$ is presented in the form of two tables, where the i -th row represents the SEDs corresponding to Hamming weight i of the binary representation for a signal point. MGF is represented by a list of nonzero probabilities and the corresponding normalized SEDs. For large signal sets only six first coefficients of MGFs are presented.

Computations show that BPCM and ASCM for 8-PAM and $q = 2^4$ are identical. Nevertheless, for practical codes simulation results differ. Notice that ASCM implies some restrictions on combination of modulation order and size of symbol alphabet, whereas BPCM is applicable for an arbitrary set of parameters.

REFERENCES

- [1] I. E. Bocharova, B. D. Kudryashov, and V. Skachek, "Euclidean distance spectra of irregular NB LDPC coded QAM signals with optimized mappings," in *Proc. IEEE Int. Symp. Inf. Theory (ISIT)*. IEEE, 2021, pp. 226–231.
- [2] I. E. Bocharova, B. D. Kudryashov, E. P. Ovsyannikov, and V. Skachek, "A random coding bound on the ML decoding error probability for NB LDPC coded QAM signals," in *IEEE Inform. Theory Workshop (ITW)*. IEEE, 2021, pp. 1–6.
- [3] M. Davey and D. J. C. Mackay, "Low density parity check codes over GF(q)," *IEEE Commun. Lett.*, vol. 2, no. 6, pp. 165–167, 1998.
- [4] C. Poulliat, M. Fossorier, and D. Declercq, "Using binary images of non binary LDPC codes to improve overall performance," in *4th Int. Symposium on Turbo Codes & Related Topics; 6th International ITG-Conference on Source and Channel Coding*. VDE, 2006, pp. 1–6.
- [5] R. G. Gallager, *Low-Density Parity-Check Codes*. M.I.T. Press: Cambridge, MA, 1963.
- [6] D. Declercq, M. Colas, and G. Gelle, "Regular GF (2^q)-LDPC modulations for higher order QAM-AWGN channels," in *Proc. Int. Symp. Inf. Theory Appl. (ISITA)*, 2004.
- [7] S. Pfletschinger, A. Mourad, E. Lopez, D. Declercq, and G. Bacci, "Performance evaluation of non-binary LDPC codes on wireless channels," in *Proc. ICT Mobile Summit*. Santander, 2009, pp. 1–8.
- [8] L. Mostari, A. Taleb-Ahmed, and A. Bounoua, "Simplified soft output demapper for non-binary LDPC codes," *Optik*, vol. 126, no. 24, pp. 5074–5076, 2015.
- [9] C. Poulliat, M. Fossorier, and D. Declercq, "Design of regular ($2, d_c$)-LDPC codes over GF(q) using their binary images," *IEEE Transactions on Communications*, vol. 56, no. 10, pp. 1626–1635, 2008.
- [10] G. Li, I. J. Fair, and W. A. Krzymien, "Density evolution for nonbinary LDPC codes under Gaussian approximation," *IEEE Trans. Inf. Theory*, vol. 55, no. 3, pp. 997–1015, 2009.
- [11] M. Arabaci, I. B. Djordjevic, R. Saunders, and R. M. M. Marcocchia, "High-rate nonbinary regular quasi-cyclic LDPC codes for optical communications," *J. of lightwave technol.*, vol. 27, no. 23, pp. 5261–5267, 2009.
- [12] G. Rezgui, A. Maaloui, I. Andryanova, and C. Poulliat, "Analysis of irregular NB LDPC coded QAM signals," in *Proc. Int. Symp. Inf. Theory Appl. (ISITA)*, Oct. 24–27 2020.
- [13] I. E. Bocharova, B. D. Kudryashov, E. P. Ovsyannikov, V. Skachek, and T. Uustalu, "Optimization of NB QC-LDPC block codes and their performance analysis," *arXiv preprint arXiv:2006.12147*, 2020.
- [14] D. Delahaye, S. Chaimatanan, and M. Mongeau, "Simulated annealing: From basics to applications," in *Handbook of Metaheuristics*. Springer, 2019, pp. 1–35.

TABLE V: MGF of normalized SEDS for selected mappings

Mapping	Parameters		Probabilities	Distances
	q	M		
BICM	–	4	3/4 1/4 1 0	4 36 8 –
BICM	–	8	7/12 1/4 1/12 1/12 1 1/2 1/3 1/6 1/2 1/2 – –	4 36 100 196 8 32 72 – 12 100/3 – –
SICM	4	4	3/4 1/4 0 0 3/8 1/3 1/4 1/24 3/4 1/4 – – 1 – – –	4 36 – – 4 8 10 18 20/3 52/3 – – 8 – – –
SICM	8	6	0.583 0.25 0.083 0.083 0 0 ... 0.207 0.203 0.177 0.135 0.038 0.0591 ... 0.276 0.053 0.118 0.184 0.132 0.0395 ... 0.158 0.123 0.053 0.211 0.123 0.0702 ... 0.25 0.167 0.25 0.167 0.083 0.0833 ... 0.25 0.5 0.25 0 0 0 ...	4 36 100 196 – –1 ... 4 8 20 32 36 52 ... 20/3 12 52/3 68/3 100/3 116/3 ... 8 10 18 20 26 32 ... 52/5 20 116/5 164/5 36 244/5 ... 12 78/3 100/3 – – – ...
BPCM, ASCM	4	8	0.583 0.25 0.083 0.083 0 0 ... 0.283 0.093 0.243 0.062 0.052 0.081 ... 0.138 0.203 0.013 0.178 0.087 0.135 ... 0.034 0.202 0.049 0.038 0.059 0.173 ... 0.11 0.162 0.063 0.031 0.141 0.069 ... 0.113 0.066 0.086 0.101 0.038 0.187 ... 0.106 0.124 0.061 0.024 0.046 0.106 ... 0.033 0.151 0.029 0.029 0.067 0.112 ... 0.093 0.109 0.007 0.047 0.186 0.072 ... 0.094 0.024 0.011 0.125 0.188 0.073 ... 0.063 0.042 0.188 0.125 0.208 0.125 ... 0.063 0.25 0.375 0.25 0.063 0 ...	4 36 100 196 – – ... 4 8 20 32 36 52 ... 4 20/3 12 44/3 52/3 68/3 ... 4 6 8 10 12 14 ... 28/5 36/5 44/5 52/5 12 68/5 ... 20/3 6 28/3 12 40/3 44/3 ... 52/7 60/7 68/7 76/7 14 92/7 ... 8 9 10 11 12 14 ... 84/9 92/9 12 124/9 44/3 140/9 ... 10.4 11.2 14.4 15.2 16.8 17.6 ... 124 172 188 236 252 300 ... 11 11 11 11 11 11 ... 12 52/3 68/3 28 100/3 – ...

- [15] I. Bocharova, B. Kudryashov, and R. Johannesson, "Searching for binary and nonbinary block and convolutional LDPC codes," *IEEE Trans. Inf. Theory*, vol. 62, no. 1, pp. 163–183, 2016.
- [16] D. Declercq and M. Fossorier, "Decoding algorithms for nonbinary LDPC codes over $GF(q)$," *IEEE Trans. Comm.*, vol. 55, no. 4, pp. 633–643, 2007.
- [17] —, "Extended minsum algorithm for decoding LDPC codes over $GF(q)$," in *Proc. IEEE Int. Symp. Inf. Theory (ISIT)*. IEEE, 2005, pp. 464–468.
- [18] V. Savin, "Min-max decoding for non binary LDPC codes," in *Proc. IEEE Int. Symp. Inf. Theory (ISIT)*. IEEE, 2008, pp. 960–964.
- [19] X. Zhang and F. Cai, "Partial-parallel decoder architecture for quasi-cyclic non-binary LDPC codes," in *2010 IEEE Intern. Conf. on Acoustics, Speech and Signal Processing*. IEEE, 2010, pp. 1506–1509.
- [20] J. O. Lacruz, F. Garcia-Herrero, D. Declercq, and J. Valls, "Simplified trellis min-max decoder architecture for nonbinary low-density parity-check codes," *IEEE Trans. on Very Large Scale Integration (VLSI) Systems*, vol. 23, no. 9, pp. 1783–1792, 2014.
- [21] G. Caire, G. Taricco, and E. Biglieri, "Bit-interleaved coded modulation," *IEEE Trans. Inf. Theory*, vol. 44, no. 3, pp. 927–946, 1998.
- [22] H. Imai and S. Hirakawa, "A new multilevel coding method using error-correcting codes," *IEEE Trans. Inf. Theory*, vol. 23, no. 3, pp. 371–377, 1977.
- [23] G. Ungerboeck, "Channel coding with multilevel/phase signals," *IEEE Trans. Inf. Theory*, vol. 28, no. 1, pp. 55–67, 1982.
- [24] F. J. MacWilliams and N. J. A. Sloane, *The theory of error-correcting codes*. Elsevier, 1977, vol. 16.
- [25] C. E. Shannon, "Probability of error for optimal codes in a Gaussian channel," *Bell System Technical Journal*, vol. 38, no. 3, pp. 611–656, 1959.
- [26] I. Sason and S. Shamai, *Performance analysis of linear codes under maximum-likelihood decoding: A tutorial*. Now Publishers Inc, 2006.
- [27] Y. Polyanskiy, H. V. Poor, and S. Verdú, "Channel coding rate in the finite blocklength regime," *IEEE Trans. Inf. Theory*, vol. 56, no. 5, pp. 2307–2359, 2010.
- [28] H. Herzberg and G. Poltyrev, "Techniques of bounding the probability of decoding error for block coded modulation structures," *IEEE Trans. Inf. Theory*, vol. 40, no. 3, pp. 903–911, 1994.

- [29] M. G. Luby, M. Mitzenmacher, M. A. Shokrollahi, and D. A. Spielman, "Efficient erasure correcting codes," *IEEE Trans. Inf. Theory*, vol. 47, no. 2, pp. 569–584, 2001.
- [30] D. Burshtein and G. Miller, "Asymptotic enumeration methods for analyzing LDPC codes," *IEEE Trans. Inf. Theory*, vol. 50, no. 6, pp. 1115–1131, 2004.
- [31] S. Litsyn and V. Shevelev, "Distance distributions in ensembles of irregular low-density parity-check codes," *IEEE Trans. Inf. Theory*, vol. 49, no. 12, pp. 3140–3159, 2003.
- [32] K. Kasai, C. Poulliat, D. Declercq, and K. Sakaniwa, "Weight distributions of non-binary LDPC codes," *IEICE Trans. Fundamentals*, vol. 94, no. 4, pp. 1106–1115, 2011.
- [33] S. Litsyn and V. Shevelev, "On ensembles of low-density parity-check codes: Asymptotic distance distributions," *IEEE Trans. Inf. Theory*, vol. 48, no. 4, pp. 887–908, 2002.
- [34] I. Andriyanova, V. Rathi, and J.-P. Tillich, "Binary weight distribution of non-binary LDPC codes," in *Proc. IEEE Int. Symp. Inf. Theory (ISIT)*. IEEE, 2009, pp. 65–69.
- [35] I. E. Bocharova, B. D. Kudryashov, V. Skachek, and Y. Yakimenka, "Average spectra for ensembles of LDPC codes and applications," in *Proc. IEEE Int. Symp. Inf. Theory (ISIT)*, 2017, pp. 361–365.
- [36] M. El-Khamy and R. J. McEliece, "Bounds on the average binary minimum distance and the maximum likelihood performance of Reed Solomon codes," in *42nd Allerton Conf. on Commun., Control and Computing*, 2004.
- [37] W. Feller, *Probability theory and its applications, vol. 1 New York*. John Wiley and Sons, Inc., 1968.